



Providing Choice & Value

Generic CT and MRI Contrast Agents



FRESENIUS
KABI

CONTACT REP

AJNR

**Inflammatory CNS Demyelination:
Histopathologic Correlation with In Vivo
Quantitative Proton MR Spectroscopy**

Andreas Bitsch, Harald Bruhn, Vassilios Vougioukas, Argyris Stringaris, Hans Lassmann, Jens Frahm and Wolfgang Brück

This information is current as
of July 31, 2025.

AJNR Am J Neuroradiol 1999, 20 (9) 1619-1627
<http://www.ajnr.org/content/20/9/1619>

Inflammatory CNS Demyelination: Histopathologic Correlation with In Vivo Quantitative Proton MR Spectroscopy

Andreas Bitsch, Harald Bruhn, Vassilios Vougioukas, Argyris Stringaris, Hans Lassmann, Jens Frahm, and Wolfgang Brück

BACKGROUND AND PURPOSE: The mechanisms behind the demyelination that is characteristic of multiple sclerosis (MS) are still poorly understood. The purpose of this study was to compare immunopathologic findings in demyelinating lesions of three patients with in vivo assessments obtained by quantitative proton MR spectroscopy (MRS).

METHODS: Between four and seven stereotactic needle brain biopsies were performed in three young adults with diagnostically equivocal findings for MS. Axonal density, gliosis, blood brain-barrier breakdown, and demyelinating activity of lesions were determined. Combined MR/MRS studies were performed (T1-weighted fast low-angle shot and single-voxel stimulated-echo acquisition mode), and absolute metabolite levels were obtained with a user-independent fitting routine. Metabolite control values were obtained from a group of age-matched healthy volunteers (n=40, age range, 20–25 years old). Alterations of metabolite levels of control subjects were considered significant when exceeding two standard deviations.

RESULTS: There were parallel decreases of *N*-acetylaspartate (21%–82%) and reductions of axonal density (44%–74%) in demyelinating plaques. Concomitant increases of choline (75%–152%) and myo-inositol (84%–160%) corresponded to glial proliferation. Elevated lactate was associated with inflammation.

CONCLUSION: The present data suggest that in vivo MRS indicates key pathologic features of demyelinating lesions.

Multiple sclerosis (MS) is a chronic inflammatory disease of the CNS characterized by focal areas of demyelination (1, 2). The mechanisms behind the destruction of myelin, however, are still poorly understood. Recent studies on oligodendrocyte pathology suggest a heterogeneous pathogenesis (3). The diagnosis of MS is generally made on the basis of clinical, laboratory, and radiologic findings. MR imaging, complemented by enhancement with the contrast agent gadolinium-diethylene-triamine pentaacetic acid (Gd-DTPA) is the method of choice for defining the location, extent, and activity of MS

lesions in the brain (4, 5). MR imaging is often implemented in therapeutic studies to define the reduction of disease activity during therapy. MR findings, however, may be nonspecific and do not necessarily allow definition of the underlying pathologic changes within a single lesion. For example, Gd-DTPA enhancement may also occur in chronic inactive lesions, and hyperintense T2 lesions may indicate inflammation as well as demyelination or axonal loss (6).

Proton MR spectroscopy (MRS) has emerged as a sensitive tool for studying the biochemical behavior of demyelinating plaques in vivo (5). Relative to normal-appearing white matter, metabolic alterations detected by proton MRS include reductions of *N*-acetylaspartate (NAA) as a putative indicator of persistent axonal damage, namely in chronic MS lesions (7–9). Moreover, choline-containing compounds (Cho) and myo-inositol (Ins) were both found to be elevated within MS plaques, suggesting enhanced membrane turnover (9–13). The rise of lactate (Lac) within some lesions may correspond to the degree of inflammation, ie, the infiltration of macrophages in the acute episodes as seen also in other cerebral diseases (12, 14).

Received in original form January 6, 1999; accepted after revision May 10, 1999.

From the Departments of Neuropathology (V.V., A.S., W.B.) and Neurology (A.B.), of Georg-August University, Göttingen, Germany; Biomedical MRI Study Group at the Max Planck Institute of Biophysical Chemistry (H.B.), Göttingen, Germany; and the Neurological Institute (H.L.), Vienna, Austria.

Address reprint requests to PD Dr. med. Wolfgang Brück, Institut für Neuropathologie, Robert-Koch-Straße 40, 37075 Göttingen, Germany.

Financial support by the Gemeinnützige Hertie-Stiftung (GHS 292/94) and the Austrian Science Foundation (Project P 10608 Med) is gratefully acknowledged.

Table 1: Synopsis of clinical and diagnostic findings.

Patient	#1	#2	#3
Age/years	20	37	21
Sex	Female	Male	Female
Clinical findings at onset	Bilateral optic neuritis, slight limb ataxia, nausea, vomiting	Hemiparesis, hypesthesia of trigeminal nerve	Hemiparesis, focal seizures, mild aphasia
CSF findings	Normal	OCB	Increased total protein
Interval from first symptoms to biopsy	2 months	7 months	7.5 months
MRI at biopsy	Bilateral large lesions, Gd+	Large parietal lesion, multiple periventricular lesions, partly Gd+	Bilateral large lesions, Gd+
Follow-up clinical data	For 6 years no further bout, no disability other than vision loss	At least 1 further bout, rapid progression of disability	Several bouts, severely disabled
Poser criteria (20)	Clinically probable MS	Laboratory-supported definite MS	Clinically definite MS
Disease course	Monophasic (so far)	Secondary progressive	Secondary progressive

So far, few studies have investigated the utility of proton MRS findings in morphologically confirmed demyelinating lesions. In fact, pertinent investigations have measured biopsy specimens (9, 12, 15, 16) or autopsy tissue from MS patients (17) in an attempt to confirm the demyelinating process rather than to relate MRS findings to detailed histopathologic and immunopathologic parameters of the plaques. Because such data are critical for the interpretation of MRS-based *in vivo* disease, the present study compares *in vivo* MRS findings to pathologic characteristics of lesions in three cases of inflammatory CNS demyelination consistent with MS, which were confirmed by biopsy.

Methods

Clinical History of Patients

This study includes three young adult patients who had been subjected to brain biopsy because of equivocal diagnostic findings that did not exclude certain treatable diseases other than MS such as lymphoma, glioma, or toxoplasmosis. The three patients were not selected on the basis of different types of disease or from a larger group of patients. The clinical history, CSF data, and MR findings were reported previously (18, 19) and are summarized in Table 1. Between four and seven stereotactic needle biopsies were taken from the left parieto-occipital white matter (case 1), right parietal white matter (case 2), and right frontoparietal white matter (case 3). Currently, the diagnosis of MS is clinically definite in two patients according to the Poser criteria (20). In one patient (case 1), however, MS is still only probable considering the lack of a second bout during the past 6 years. No patient received steroids or any immunosuppressive treatment prior to biopsy. All patients were prescribed a course of steroids after biopsy, which ended at least 2 weeks before MRS for cases 2 and 3, whereas case 1 still received 35 mg/d prednisolone at the time of the MRS examination. Time elapsed between biopsy and subsequent MRS examination of the patients was 6 weeks in case 1, 11 and 17 weeks in case 2, and 21 weeks in case 3.

Neuropathologic Analysis

Paraffin-embedded biopsy material, which had been collected at the Department of Neuropathology of the Georg-August University at Göttingen, was used. Sections were stained with hematoxylin and eosin (H&E), Luxol fast blue (LFB), periodic acid-Schiff (PAS), and Bielschowsky's silver impregnation.

Immunocytochemical Analysis

Immunocytochemical analysis was performed with a biotin-avidin or an alkaline phosphatase/anti-alkaline phosphatase technique. The following primary antibodies were used (see reference 19 and 21).

Myelin/oligodendrocytes.—Anti-myelin basic protein (MBP, Boehringer Mannheim, Mannheim, Germany), anti-proteolipid protein (PLP), and anti-myelin oligodendrocyte glycoprotein (MOG) were used. The latter was provided by Dr. Piddlesden (University of Cardiff, UK).

Monocytes/macrophages.—Anti-Ki-MIP was provided by Dr. Radzun (University of Göttingen, Germany). We also used anti-27E10, anti-MRP14, anti-25F9, and anti-MRP8 (BMA Biomedicals, August, Switzerland).

T cells.—Anti-CD3, (Dako, Denmark) was used.

Astrocytes.—Anti-glial fibrillary acid protein (GFAP) (Dako, Denmark) was used.

Immunoglobulins.—Anti-human IgG (Dako, Denmark) was used.

In Situ Hybridization

For *in situ* hybridization, digoxigenin-labeled riboprobes specific for PLP mRNA were used (22). The source and specificity of the probes, the labeling techniques, and the methods of *in situ* hybridization have been described in detail (23).

Axonal Density, Gliosis, Edema, and Blood Brain-Barrier Breakdown

Axonal density was determined in sections stained with Bielschowsky's silver impregnation by point sampling using a 24-point Zeiss eyepiece (24). Measurements of all lesions were performed at an identical final magnification of $\times 800$ to guarantee comparability. Random points were superimposed on the plaques and the periplaque white matter. The number of points crossing axons was measured as a fraction of the total number of points on the stereologic grid. A recent study confirmed the reliability of this method for quantifying axonal density in different regions of the cerebral white matter (24). Axonal density is expressed as the percentage of reduction compared with the periplaque white matter (Fig 1A–C).

Gliosis was determined in sections stained for GFAP. Protoplasmic gliosis with large swollen astrocytes was distinguished from fibrillary gliosis with dense glial scarring (Fig 1D–E). Blood brain-barrier (BBB) breakdown was assessed in sections stained for human IgG. Moderate or severe protein extravasation was distinguished. The degree of extracellular edema (moderate or severe) was defined as the widening of the extracellular space within the lesions. Severe edema resulted in the formation of a vacuolated extracellular space. Gli-

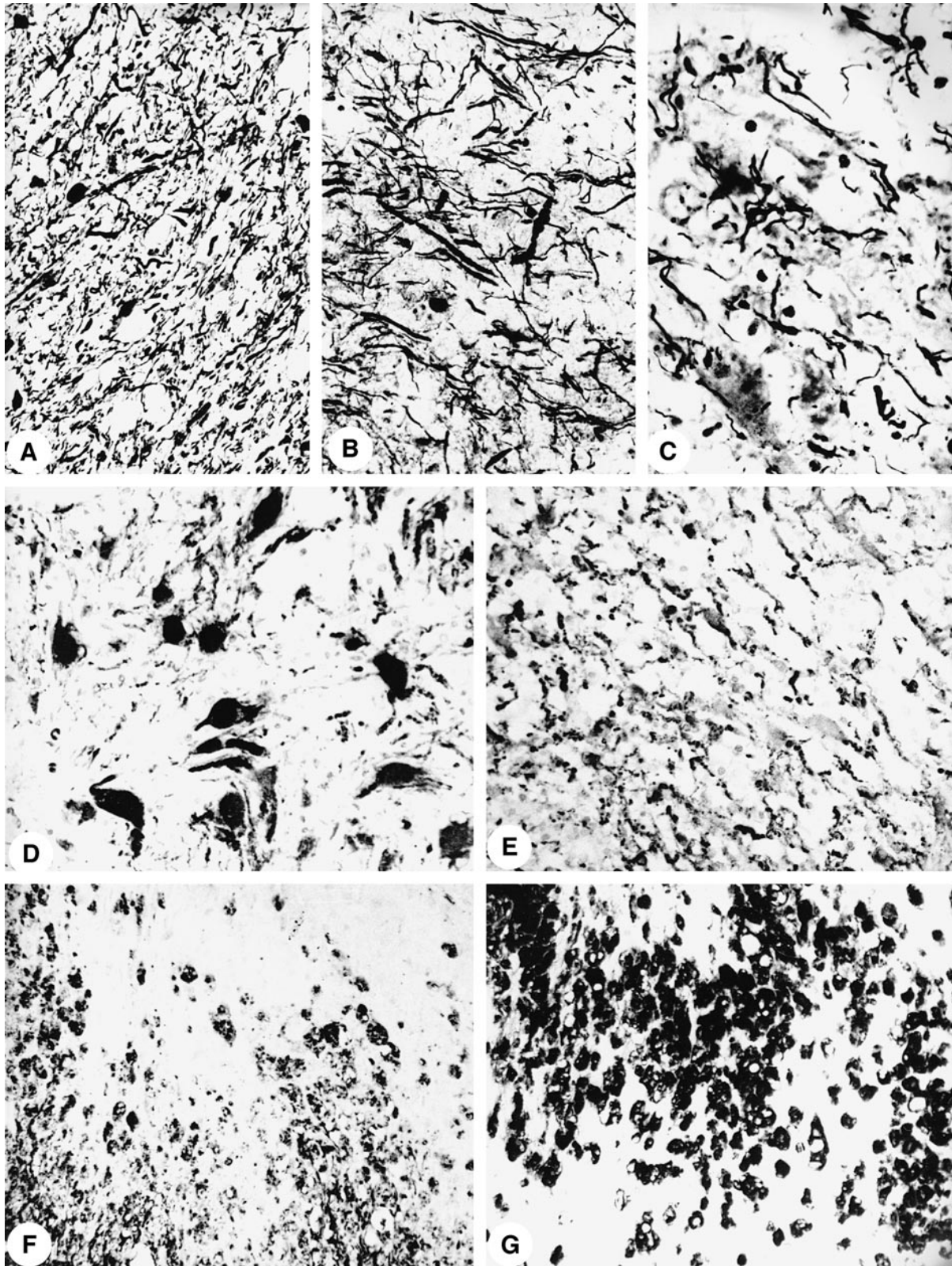


FIG 1. Bielschowsky's silver impregnation shows axonal density in the normal periplaque white matter (patient 1) (A), a reduction by 45% (patient 3) (B), and a reduction by 75% (patient 1) (C) within the plaques (magnification for all, $\times 166$). Prominent protoplasmic gliosis with large astrocytes (D) is seen by immunocytochemistry for GFAP (patient 1). Numerous GFAP-positive cell processes (E) indicate fibrillary gliosis (patient 3). Immunocytochemistry for MOG (F) shows an early active demyelinating lesion (patient 2). Macrophages carry MOG-positive degradation products in their cytoplasm. Dense macrophage infiltrate (G) is seen in the same lesion as shown in F (immunocytochemistry for Ki-MIP).

Table 2: Lesion histopathology and corresponding proton MRS-detected metabolic alterations. Absolute metabolite levels (mM/L VOI) derived from proton MR spectra (STEAM, TR/TE/TM = 3000/20/30 ms) of biopsied lesions of patients #1 to #3.

Patient Lesional activity	#1 ERM/LRM	#2 EA/LA	#3 DM	#1-3 NAWM
Axonal damage				
Axon reduction*	-63%	-44%	-74%	0
NAA [mM] (6.5 ± 0.7 mM)‡	1.2 2.4	5.1	2.9	6.1-9.4
Relative NAA§	-63/-82%	-21%	-55%	
Edema [¶]	+	++	+	-
Astrocyte proliferation				
Gliosis	Protoplasmatic/fibrillary	Protoplasmatic	Fibrillary	-
Cho [mM] (1.2 ± 0.2 mM)‡	3.0 2.4	2.4	3.1	0.5
Relative Cho§	+100/150%	+100%	+152%	
Ins [mM] (2.5 ± 0.6 mM)‡	6.2 5.2	4.6	6.5	2.7 5.8
Relative Ins§	+108/148%	+84%	+160%	
Inflammation				
Macrophages/mm ²	688	1316	1084	8-100
Macrophage activation [¶]	-	+	-	-
Lac [mM] (≤0.5 mM)‡	4.7 3.0	4.9	2.5	0.5

* Percentage reduction/increase in comparison to periplaque white matter. ‡ controls (n = 20; white matter, VOI = 12 ml, mean ± SD); § Percentage changes in comparison to normal controls; ¶ + = moderate; ++ = severe; - = none; || Values correspond to a large/small VOI of the same lesion. VOI's for spectroscopy range from 4.1-8.0 ml. EA = early active lesion; LA = late active lesion; DM = demyelinated lesion; ERM = early remyelinating lesion; LRM = late remyelinating lesion; NAWM = normal appearing white matter.

osis, BBB breakdown, and extracellular edema were determined at the same final magnification.

Morphometric Analysis

The number of oligodendrocytes (MOG immunocytochemistry or PLP mRNA in situ hybridization), T cells (CD3 immunocytochemistry), and macrophages (KiMIP immunocytochemistry) stained per square unit of tissue was determined on serial sections selected according to the demyelinating activity within the plaques (see Results). The number of cells was determined in at least 10 standardized microscopic fields of 10,000 μm^2 each that were defined by an ocular morphometric grid. The values are summarized in Table 2 as the number of cells per mm^2 .

MR Spectroscopy

Combined MR/MRS studies were performed on a 2-T imaging unit (Magnetom SP4000, Siemens Erlangen, Germany) using the standard imaging head coil. Image-guided selection of a volume of interest (VOI) for proton MRS was based on T1-weighted fast-low-angle-shot images. Short-echo-time proton MR spectra (3000/20/30 [TR/TE/TM], 128 accumulations) were acquired using a single-voxel stimulated-echo acquisition-mode localization sequence as described previously (25). VOIs were placed to include lesions, defined as areas of T1-weighted signal decrease, as well as unsuspected white matter in small paraventricular locations to allow for intrasubject comparisons. "Gray matter" spectra were obtained from VOIs placed symmetrically around the sagittal fissure.

Data evaluation comprised a correction of the spectroscopic time-domain data for residual eddy current effects and calibration of signal intensities in proportion to the actual coil loading to account for intersubject sensitivity differences. For display purposes only, spectral postprocessing involved zero-filling to 4 K complex data points (2048 ms), Gaussian filtering (half-width 317 ms), and manual-phase correction. Absolute metab-

olite levels were obtained with LCModel, a user-independent fitting routine based on a library of model spectra of all individual metabolites (26-28). Concentration values are expressed as mmol/L VOI (mM) and are not corrected for contributions by CSF and a small reduction of the numerical values by residual T1 and T2 relaxation effects.

Metabolite control values were obtained from a group of age-matched healthy volunteers (n = 40; age range, 20-35 years) investigated at the time of the patient measurements with the same methodology. Apart from different T1 relaxation weightings, the results were in general agreement with a more recent study of young subjects performed in this laboratory (28). Alterations of metabolite levels from those of control subjects were considered significant when exceeding two standard deviations.

Results

Neuropathologic Findings

A total of 15 serial stereotactic needle biopsy specimens (four to seven per patient) from different plaque areas were available. All specimens contained demyelinated tissue in various stages of demyelinating activity as well as areas of remyelination. A total of 18 lesions in different stages of demyelinating activity were studied as defined below. Additionally, four areas of periplaque white matter were analyzed. Histologic characteristics of MS plaques included inflammation and a certain degree of either fibrillary or protoplasmic astrocytic gliosis (Fig 1D-E), which were both present in all samples. Oligodendrocytes were largely preserved within the lesions and exhibited only a minor reduction compared with the periplaque white matter.

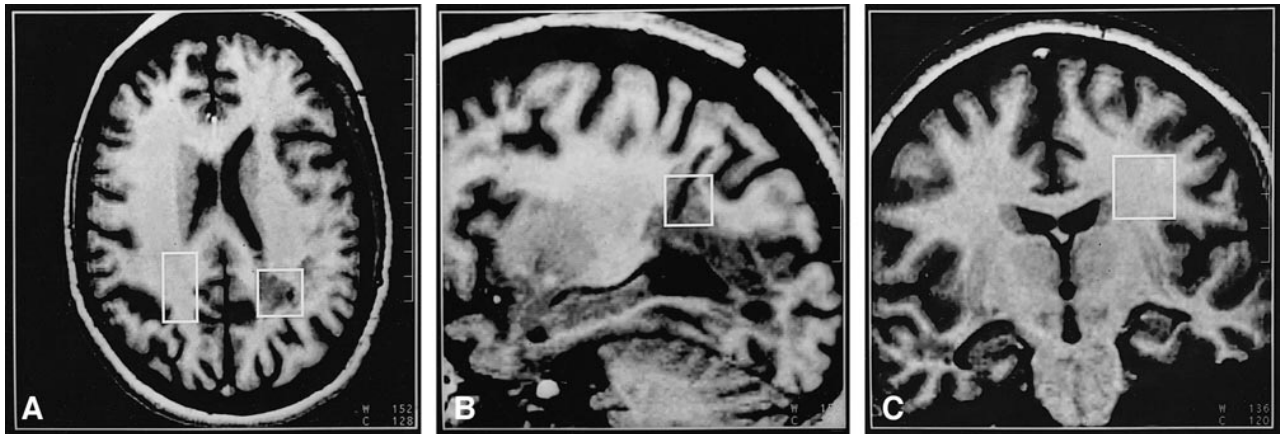


FIG 2. T1-weighted gradient-echo MR images (3D fast low-angle shot, 4-mm partitions, 15/6 TR/TE, 20° flip angle) of patient 1 indicating VOIs selected for MRS.

A, Transverse section with VOIs centered at the left parieto-occipital lesion ($20 \times 20 \times 20 \text{ mm}^3$) and in a contralateral control region ($16 \times 30 \times 16 \text{ mm}^3$).

B, Sagittal section with a smaller VOI ($16 \times 16 \times 16 \text{ mm}^3$) encompassing the same lesion (note small defect in the skull and corresponding biopsy canal).

C, Coronal section depicting an ipsilateral VOI ($20 \times 20 \times 20 \text{ mm}^3$) in left frontoparietal cortex unsuspecting at MR imaging.

Demyelinated plaques were infiltrated by numerous macrophages (Fig 1G). Macrophage activation was defined by the expression of MRP14 and 27E10 and was detected in actively demyelinating lesions. Axonal density was more reduced in all lesions than it was in periplaque white matter (Fig 1A–C). Edema was present in all lesions but not in the periplaque white matter. There was no systematic relationship between the degree of edema and axonal density.

Definition of Demyelinating Activity

According to the presence of myelin degradation products in the macrophage cytoplasm and the expression of macrophage activation antigens (19,21), the following stages of demyelinating activity were distinguished.

Early active lesions.—Early active lesions (patient 2 [n=4]) were located at the border between demyelinated plaques and periplaque white matter. Macrophages contained myelin degradation products that were stained with LFB and were immunoreactive for all myelin proteins, including MOG (Fig 1F). The macrophages expressed the acute stage inflammatory macrophage markers MRP14 and 27E10.

Late active lesions.—Myelin degradation (patient 2 [n=3]) was more advanced in late active lesions. Macrophages diffusely infiltrated the lesion and contained myelin degradation products with immunoreactivity for the major myelin proteins MBP or PLP but not for MOG. Macrophages still expressed the acute stage inflammatory marker 27E10.

Inactive demyelinated lesions.—These lesions (patient 3 [n=4]) were infiltrated by macrophages, which contained either empty vacuoles or PAS-positive degradation products and expressed the

chronic-stage inflammatory macrophage marker 25F9.

Early remyelinating lesions.—Early remyelinated lesions (patient 3 [n=1]) were infiltrated by numerous lymphocytes and macrophages and showed clusters of axons surrounded by thin myelin sheaths.

Late remyelinating lesions.—Only few macrophages were present in these lesions (shadow plaques, patient 1 [n=3]). The axons were surrounded by thin myelin sheaths, and fibrillary gliosis was prominent.

Proton MRS Findings

As a typical example, Figure 2 shows selective T1-weighted MR sections for patient 1 to indicate the location and size of the VOIs chosen for MRS. They demonstrate the demarcation of the demyelinating disease (Gd-DTPA enhancement on MR images 12 days before biopsy) by signal decreases. The corresponding proton MR spectra in Figure 3 display the prominent single resonances of NAA, creatine and phosphocreatine (Cr), choline-containing compounds, the coupled resonances for Ins and Lac, and unresolved resonances from unassigned methyl (0.8–0.9 ppm) and methylene (1.2–1.3 ppm) groups.

Table 2 summarizes the absolute metabolite levels for all three patients derived from proton MRS in vivo as well as mean white matter values for a group of age-matched control subjects. In particular, for the small VOI of the biopsied lesion in case 1, proton MRS revealed a greater than fivefold reduction of NAA (1.2 versus 6.5 mM), a greater than twofold increase of both Cho (3.0 versus 1.2 mM) and Ins (6.2 vs. 2.5 mM), and a marked increase of Lac (4.7 mM). All changes clearly exceeded two standard deviations of control values.

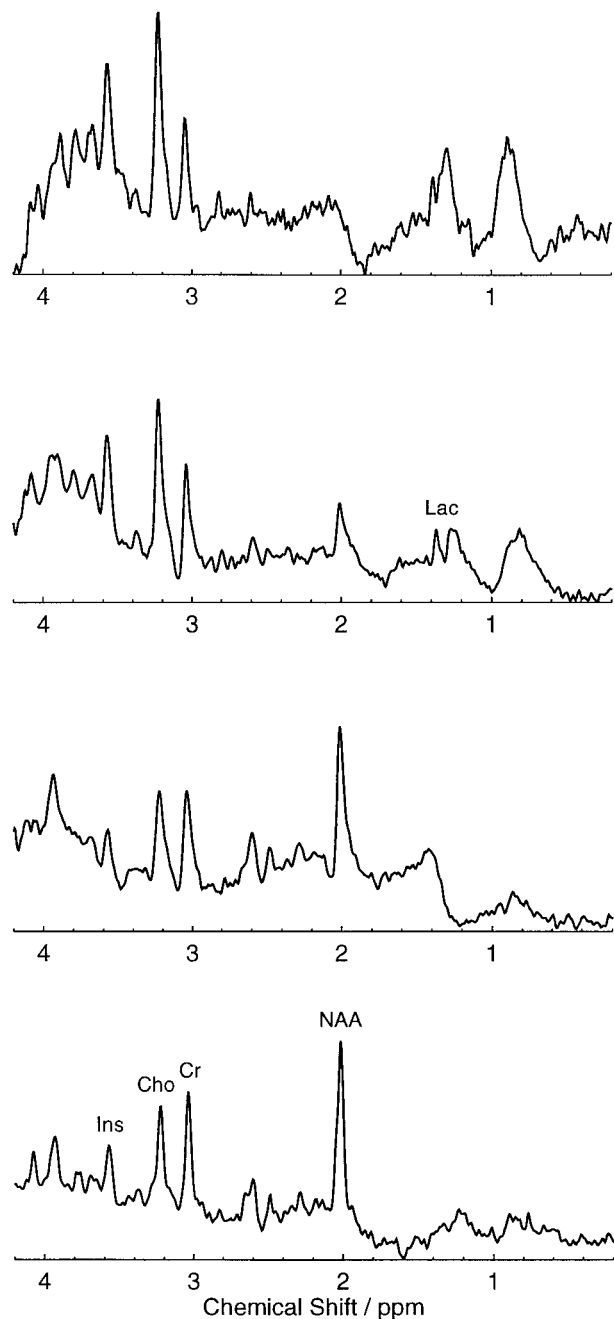


FIG 3. Localized proton MR spectra (stimulated-echo acquisition mode, 3000/20/30 [TR/TE/TM]) of patient 1 from locations indicated in Figure 2. Left occipitoparietal lesion (*top*) image using a 4-mL VOI and (*second row*) 8-mL VOI, an ipsilateral 8-mL VOI in unsuspecting left frontoparietal cortex (*third row*), and contralateral control (*bottom*). Major resonances are due to N-acetylaspartate (NAA), creatine and phosphocreatine (Cr), choline-containing compounds (Cho), myo-inositol (Ins), and lactate (Lac). Spectra are normalized for comparison.

In this case, a larger VOI (double size) also was investigated to demonstrate the extent to which the partial voluming of visible lesion and surrounding normal-appearing white matter affects the measured metabolite concentrations. That is, the absolute NAA decreased, and the Cho and Ins increase appeared less marked with increasing partial vol-

uming. By volumetric assessment, normal-appearing white matter contributed only below 10% for the smaller VOI and up to 20% for the larger VOI of this case. As seen on the images, the defect caused by the biopsy canals also contributed to the VOIs (up to 15%). Similar to CSF spaces, however, this led to an equal decrease of all metabolites, which ultimately did not affect the relative metabolite pattern. Similar considerations with a similar magnitude of partial volume effects apply for the VOIs chosen in cases 2 and 3. Similar findings were obtained when the metabolic alterations in the lesion were compared to values obtained in contralateral white matter or ipsilateral frontoparietal white matter. Both regions appeared normal at MR, and the MRS-detected metabolite levels were within normal ranges.

The lesion of case 2 (frontal part) showed only a slight reduction of NAA (5.1 versus 6.5 mM), but again a twofold increase of Cho and Ins, and a markedly increased Lac (4.9 mM). An MRS follow-up 6 weeks later revealed a decreased Lac level (2.8 mM), but only subtle changes for the other metabolites within the limits of experimental uncertainty. Nevertheless, the trend toward normal Lac levels would comply with a recovery process that includes an abatement of inflammation. In this patient, normal-appearing white matter in two contralateral locations also was affected by increases of Cho (1.6–1.7 versus 1.2 mM), Ins (4.4–5.8 versus 2.5 mM), and Cr (5.2–5.7 versus 3.8 mM). Compared with healthy volunteers, this indicates an increase of 33% to 42% (Cho), 76% to 132% (Ins), and 37% to 50% (Cr).

In case 3, the biopsied lesion showed a twofold decrease of NAA and elevated Lac (2.5 mM). Patient 3 had the highest Cho and Ins levels of the three patients studied, reaching 152% (Cho) and 160% (Ins) of the levels found in control subjects.

No significant changes were found in the midline parietal gray matter of MS patients compared with control subjects. Nevertheless, there was a trend toward slightly increased levels of Cho. Total Cr levels within lesions showed no statistically significant deviations from control subjects; ie, 3.8 ± 0.5 mM for white matter.

Correlation of Neuropathologic Results and MR Spectra

Enumeration of axons revealed a substantial axonal loss in all MS lesions compared with periplaque white matter. Correspondingly, there was a decrease of NAA levels within the lesions as determined by MRS (Table 2). In case 1, NAA levels decreased by 63% to 82% (depending on VOI size) as compared with histopathologic reduction of the axonal density by 63% (compared with periplaque white matter). Similarly, in cases 2 and 3, NAA decreases of 21% and 55% corresponded to a reduction of axonal density by 44% and 74%, respectively. No NAA reduction was found in nor-

mal-appearing white matter. All MRS examinations of biopsied lesions exhibited marked increases of the absolute Cho (75%–152%) and Ins (84%–160%) levels (Table 2). The most pronounced increases occurred in demyelinating lesions with predominant fibrillary gliosis (patient 3). With protoplasmic gliosis becoming more prominent in remyelinating (patient 1) and active demyelinating (patient 2) lesions, Cho and Ins levels were found less elevated. Lac elevations of up to 4.9 mM, compared with a maximal level of 0.5 mM in control subjects, were identified in MS lesions (Table 2). The highest Lac levels were found in lesions with high inflammatory activity rather than in inactive demyelinated plaques, with only a few infiltrating mononuclear cells. In contrast, total Cr levels showed no statistically significant deviations from control subjects in the lesions investigated. In the normal-appearing white matter of patient 2, which was affected by glial abnormalities as evidenced by marked increases of Cho and Ins, the Cr levels also were increased beyond normal.

Discussion

A central finding of this study is the relationship between the MRS-detected decrease of NAA in MS lesions and the relative axonal density in Bielschowsky's silver stains of corresponding biopsy specimens. Notwithstanding uncertainties in matching the actual sample volumes selected for MRS and biopsies, as well as the influence of edema, these results must be taken as strong support for the interpretation of the NAA level as an indicator of the degree of neuroaxonal integrity. Additional findings include increased Cho and Ins levels that may correspond to glial cell proliferation and elevated Lac, which was most prominent in the most active stages of inflammatory demyelination.

Each of the three patients investigated suffered from inflammatory demyelination as revealed by pathologic analysis. The initial clinical course and MR findings were not typical for multiple sclerosis, which was the reason for brain biopsy. Two of three patients developed a relapsing-remitting course and the diagnosis of multiple sclerosis became clinically definite (3). One patient has remained in a stable condition for 7 years and therefore does not fulfill the criteria of definite multiple sclerosis. Nevertheless, beyond the more or less typical clinical syndrome, the variability of demyelinating lesions as revealed by histopathologic analysis and spectroscopy may be even more important. Recent immunopathologic studies clearly showed heterogeneity in the pathologic structure of actively demyelinating plaques, suggesting that different mechanisms of demyelination may occur in different MS patients, independent of clinical course. When multiple lesions from a single patient were analyzed, very uniform patterns of inflammation, demyelination, oligodendrocyte disease, axonal loss, and remyelination were found. A high

variability of lesional structure, however, was observed among different MS patients (3). This may indicate that the findings from the cases presented herein should be useful as a baseline for further studies on the pathologic behavior of MS lesions as revealed by MRS.

It is generally accepted that there is axonal damage or transection and subsequent neuronal loss in MS plaques (29, 30). These findings are supported by previous MRS investigations describing NAA reductions as a main feature of demyelinating and neurometabolic disease (14). Other MRS studies of MS biopsies or autopsies also reported NAA losses but did not relate these findings quantitatively to the axonal density within the plaques (9, 12, 15, 17). Because NAA appears to be a measure of neuroaxonal damage, it is an important predictor of neuronal dysfunction and shows a strong correlation with the patient's disability (9, 31). A persistent NAA decrease associated with no recovery of clinical symptoms may indicate irreversible axonal damage (8). Beyond reduced NAA levels within MS plaques, NAA decreases of 10% to 20% have also been claimed for normal-appearing white matter (12, 32). In our patients, no such alterations were observed relative to data obtained from control subjects, indicating the presence of intact axons within the normal-appearing white matter.

In contrast to NAA, levels of Cho were markedly increased in all lesions. This increase was more pronounced in inactive lesions with fibrillary gliosis than in active demyelinating lesions that revealed protoplasmic gliosis. In cell culture, choline-containing compounds were preferentially located in oligodendrocytes and astrocytes (33). Their increase in cerebral pathologic processes observed *in vivo* has been associated with increased membrane turnover, eg, in glial proliferation (14, 34). Major components of the Cho resonance are choline-containing compounds with small molecular weight, such as phosphocholine and glycerophosphocholine (35), that form a pool involved in membrane synthesis and degradation. In contrast to phosphatidylcholine, such components have sufficiently long relaxation times to be detected under the present experimental conditions (36). Most authors report an early Cho increase in MS lesions or an elevated Cho/Cr ratio or both that may or may not return to normal during subsequent months (9, 12, 32, 37). A study of experimental allergic encephalomyelitis in guinea pigs attributed increases in Cho/Cr to inflammatory infiltration alone and found no significant contribution by demyelination upon histologic study (38). Hence, the increase in Cho would originate exclusively from an import of choline oxidase within infiltrated macrophages and lymphocytes into the lesion. Herein, the observation of marked Cho increases in connection with fibrillary gliosis suggests that the formation of fibrillary glial processes may be a major factor of Cho elevation in MS. Because, however, Cho was also increased during active demyelination and re-

myelination, in which fibrillary gliosis is much less prominent, these observations suggest the importance of at least two different processes during MS plaque evolution: inflammatory cellular infiltration as well as increased membrane turnover associated with fibrillary gliosis and possibly demyelination.

In agreement with recent proton MRS and MR studies revealing metabolic but no morphologic alterations of normal-appearing white matter in patients with MS (39, 40), one of our patients (case 2) revealed strong increases of Cho, Ins, and Cr in the contralateral white matter, indicating pronounced gliosis. Because no NAA decrease was found, and consistent with the observation of elevated Cr that was present in both glial and neuronal cells, glial proliferation seemed to precede neuroaxonal damage and MR-detectable lesion evolution. Of note, as the disease progressed, this patient developed contralateral lesions that were apparent with Gd-DTPA enhancement during MR imaging.

Similar to Cho, Ins levels were increased in all lesion types and displayed higher levels in fibrillary than in protoplasmic gliosis. According to proton MRS studies of cell cultures, Ins originates almost exclusively from glial cells (41). Other studies related elevated Ins to the acute stage of active myelin breakdown (9, 13, 15, 42). We, however, found it elevated also in inactive demyelinated lesions without evidence of myelin phagocytosis. Consistent with previous MRS studies of brain disorders and, in particular, with common and opposing alterations of Cho and Ins levels in demyelinating and hypomyelinating diseases (14, 43), the present findings of elevated Ins most likely represent both the accumulation of myelin breakdown products during acute phases and astrocytosis in demyelinated and remyelinated lesions. This also applies to abnormal Ins levels in normal-appearing white matter (case 2).

Although Cr levels within biopsied lesions were normal compared with controls, they were increased in the normal-appearing white matter of patient 2, which was affected by glial abnormalities as evidenced by concomitant increases of Cho and Ins. This finding is in line with investigations of metabolite ratios measured by proton MR spectroscopic imaging that report an increase of Cr in and around T1 hypointensities in relapsing-remitting MS (39, 44). It may best be understood as a higher density of cells per spectroscopic VOI that results from glial proliferation in the presence of still-intact neuroaxonal structures. In fact, both neuronal and glial cells harbor Cr compounds for their cellular homeostasis and energy needs. Further support for this interpretation stems from the fact that we made similar observations of elevated Cho (58%), Ins (112%), and Cr (58%) in one lesion with normal NAA that was not biopsied in case 2. Thus, the finding of more or less normal Cr levels in MS lesions may be an "artifact" resulting from counterbalancing effects of neuroaxonal loss and glial proliferation.

The large lesions studied herein also displayed notable Lac elevations that were identified by chemical shift and the typical coupling constant of 7 Hz. Because the dominant bioenergetic pathway in activated macrophages has been shown to be glycolysis (45), this finding would indicate an inflammatory process with cellular infiltration, as noted by others (12). Histologic findings of activated macrophages in lesions with highest Lac levels are consistent with this view. Lac generation after biopsy injury, however, might be considered, but this should involve inactive lesions to a similar extent. Because of neuronal mitochondrial injury, increased glycolysis may be another source of Lac (16).

The occurrence of broad resonances in the aliphatic methyl and methylene region in proton MR spectra of MS plaques is often ascribed to the presence of mobile lipids, (eg, compare the top [lesion] and bottom spectra [control subject] [Fig 3]). Although minor contributions from very short-chain fatty acids cannot entirely be excluded, the spectral structure of these resonances hints at the prevalence of mobile methyl and methylene residues from cytosolic proteins. It is likely that such proteins as well as cholesterol (~0.9 ppm) become elevated either as a result of cellular disruption or during the course of cellular proliferation and growth.

In conclusion, the comparison of biochemical findings by quantitative proton MRS, with histologic features of biopsy material in three cases of demyelinating disease, demonstrate that in vivo assessments provide parallel as well as complementary information as to the histopathologic and pathophysiologic features of a single MS lesion. Pertinent data help to guide the interpretation of spectroscopic findings in terms of the cellular composition and metabolism within MS plaques.

Acknowledgments

We thank Xiangling Mao for developing data processing software.

References

1. Lassmann H. *Comparative Neuropathology of Chronic Experimental Allergic Encephalomyelitis and Multiple Sclerosis*. Berlin, Heidelberg: Springer-Verlag; 1983
2. Prineas J. W. **The neuropathology of multiple sclerosis**. In: Koetsier, J. C. *Demyelinating Diseases*. Amsterdam: Elsevier Science Publishers; 1985;8:213-257
3. Lucchinetti CF, Brück W, Rodriguez M, Lassmann H. **Distinct patterns of Multiple Sclerosis pathology indicates heterogeneity in pathogenesis**. *Brain Pathol* 1996;6:259-274
4. McDonald WI, Miller DH, Barnes D. **The pathological evolution of multiple sclerosis**. *Neuropathol Appl Neurobiol* 1992;18:319-334
5. Miller DH, Grossman RI, Reingold SC, McFarland HF. **The role of magnetic resonance techniques in understanding and managing multiple sclerosis**. *Brain* 1998;121:3-24
6. Brück W, Bitsch A, Kolenda H, Brück Y, Stiefel M, Lassmann H. **Inflammatory central nervous system demyelination: correlation of magnetic resonance imaging findings with lesion pathology**. *Ann Neurol* 1997;42:783-793
7. Arnold DL, Matthews PM, Francis G, Antel J. **Proton magnetic resonance spectroscopy of human brain in vivo in the evalu-**

- ation of multiple sclerosis: assessment of the load of disease.** *Magn Reson Med* 1990;14:154-159
8. Davie CA, Barker GJ, Webb S, et al. **Persistent functional deficit in multiple sclerosis and autosomal dominant cerebellar ataxia is associated with axon loss.** *Brain* 1995;118:1583-1592
 9. De Stefano N, Matthews PM, Antel JP, Preul M, Francis G, Arnold DL. **Chemical pathology of acute demyelinating lesions and its correlation with disability.** *Ann Neurol* 1995;38:901-909
 10. Bruhn H, Gyngell ML, Merboldt KD, Hänicke W, Frahm J. **Non-invasive assessment of brain lesions by fast scan MRI and localized proton spectroscopy.** *Neuroradiology* 1991;33:S279-S281
 11. Bruhn H, Frahm J, Merboldt KD, et al. **Multiple sclerosis in children: cerebral metabolic alterations monitored by localized proton magnetic resonance spectroscopy in vivo.** *Ann Neurol* 1992;32:140-150
 12. Arnold DL, Matthews PM, Francis GS, O'Connor J, Antel JP. **Proton magnetic resonance spectroscopic imaging for metabolic characterization of demyelinating plaques.** *Ann Neurol* 1992;31:235-241
 13. Koopmans RA, Li DKB, Zhu G, Allen PS, Penn A, Paty DW. **Magnetic resonance spectroscopy of multiple sclerosis: in-vivo detection of myelin breakdown products.** *Lancet* 1993;341:631-632
 14. Frahm J, Hanefeld F. **Localized proton magnetic resonance spectroscopy of brain disorders in childhood.** In: Bachelard, H. S. *Magnetic Resonance Spectroscopy and Imaging in Neurochemistry.* New York: Plenum Press 1997;12:329-402
 15. Kim MO, Lee SA, Choi CG, Huh JR, Lee MC. **Balo's concentric sclerosis: a clinical case study of brain MRI, biopsy, and proton magnetic resonance spectroscopic findings.** *J Neurol Neurosurg Psych* 1997;62:655-658
 16. Silver NC, Barker RA, MacManus DG, et al. **Proton magnetic resonance spectroscopy in a pathologically confirmed acute demyelinating lesion.** *J Neurol* 1997;244:204-207
 17. Davies SEC, Newcombe J, Williams SR, McDonald WI, Clark JB. **High resolution proton NMR spectroscopy of multiple sclerosis lesions.** *J Neurochem* 1995;64:742-748
 18. Poser S, Lüer W, Bruhn H, Frahm J, Brück Y, Felgenhauer K. **Acute demyelinating disease. Classification and non-invasive diagnosis.** *Acta Neurol Scand* 1992;86:579-585
 19. Brück W, Porada P, Poser S, et al. **Monocyte/macrophage differentiation in early multiple sclerosis lesions.** *Ann Neurol* 1995;38:788-796
 20. Poser CM, Paty DW, Scheinberg L, et al. **New diagnostic criteria for multiple sclerosis: guidelines for research protocols.** *Ann Neurol* 1983;13:227-231
 21. Brück W, Schmied M, Suchanek G, et al. **Oligodendrocytes in the early course of multiple sclerosis.** *Ann Neurol* 1994;35:65-73
 22. Colman DR, Kreibich G, Frey AB, Sabatini DD. **Synthesis and incorporation of myelin polypeptides into CNS myelin.** *J Cell Biol* 1982;95:598-608
 23. Breitschopf H, Suchanek G, Gould RM, Colman DR, Lassmann H. **In situ hybridization with digoxigenin-labeled probes: sensitive and reliable detection method applied to myelinating rat brain.** *Acta Neuropathol* 1992;84:581-587
 24. Mews I, Bergmann M, Bunkowski S, Gullotta F, Brück W. **Oligodendrocyte and axon pathology in clinically silent multiple sclerosis lesions.** *Multiple Sclerosis* 1998;4:55-62
 25. Frahm J, Michaelis T, Merboldt KD, Bruhn H, Gyngell ML, Hänicke W. **Improvements in localized ¹H-NMR spectroscopy of human brain. Water suppression, short echo times, and 1 mL resolution.** *J Magn Reson* 1990;1990:464-473
 26. Michaelis T, Merboldt K-D, Bruhn H, Hänicke W, Frahm J. **Absolute concentrations of metabolites in the adult human brain in vivo: quantification of localized proton MR spectra.** *Radiology* 1993;187:219-227
 27. Provencher SW. **Estimation of metabolite concentrations from localized in vivo proton NMR spectra.** *Magn Reson Med* 1993;30:672-679
 28. Pouwels PJW and Frahm J. **Regional metabolite concentrations in human brain as determined by quantitative localized proton MRS.** *Magn Reson Med* 1998;39:53-60
 29. Ferguson B, Matyszak MK, Esiri MM, Perry VH. **Axonal damage in acute multiple sclerosis lesions.** *Brain* 1997;120:393-399
 30. Trapp BD, Peterson J, Ransohoff RM, Rudick R, Mork S, Bo L. **Axonal transection in the lesions of multiple sclerosis.** *New Engl J Med* 1998;338:278-285
 31. De Stefano N, Matthews PM, Narayanan S, Francis GS, Antel JP, Arnold DL. **Axonal dysfunction and disability in a relapse of multiple sclerosis: longitudinal study of a patient.** *Neurology* 1997;49:1138-1141
 32. Davie CA, Hawkins CP, Barker GJ, et al. **Serial proton magnetic resonance spectroscopy in acute multiple sclerosis lesions.** *Brain* 1994;117:49-58
 33. Urenjak J, Williams SR, Gadian DG, Noble M. **Proton magnetic resonance spectroscopy unambiguously identifies different neural cell types.** *J Neurosci* 1993;13:981-989
 34. Bruhn H, Frahm J, Gyngell ML, et al. **Noninvasive differentiation of tumors with use of localized H-1 MR spectroscopy in vivo: initial experience in patients with cerebral tumors.** *Radiology* 1989;172:541-548
 35. Jimenez JV, Richards TL, Heide AC, Grierson JR, Shankland EG. **Incorporation of a phosphonium analogue of choline into the rat brain as measured by magnetic resonance spectroscopy.** *Magn Reson Med* 1995;33:285-292
 36. Frahm J, Bruhn H, Gyngell ML, Merboldt KD, Hänicke W, Sauter R. **Localized proton NMR spectroscopy in different regions of the human brain in vivo: relaxation times and concentrations of cerebral metabolites.** *Magn Reson Med* 1989;11:47-63
 37. Matthews PM, Francis G, Antel J, Arnold DL. **Proton magnetic resonance spectroscopy for metabolic characterization of plaques in multiple sclerosis.** *Neurology* 1991;41:1251-1256
 38. Brenner RE, Munro PMG, Williams SCR, et al. **The proton NMR spectrum in acute EAE: the significance of the change in the Cho:Cr ratio.** *Magn Reson Med* 1993;29:737-745
 39. Husted CA, Goodin DS, Hugg JW, et al. **Biochemical alterations in multiple sclerosis lesions and normal-appearing white matter detected by in vivo ³¹P and ¹H spectroscopic imaging.** *Ann Neurol* 1994;36:157-165
 40. Matthews PM, Pioro E, Narayanan S, et al. **Assessment of lesion pathology in multiple sclerosis using quantitative MRI morphometry and magnetic resonance spectroscopy.** *Brain* 1996;119:715-722
 41. Brand A, Richter-Landsberg C, Leibfritz D. **Multinuclear NMR studies on the energy metabolism of glial and neuronal cells.** *Dev Neurosci* 1993;15:189-198
 42. Landtblom A-M, Sjöqvist L, Söderfeldt B, Nyland H, Thuomas K-A. **Proton MR spectroscopy and MR imaging in acute and chronic multiple sclerosis—ringlike appearances in acute plaques.** *Acta radiol* 1996;37:278-287
 43. Pouwels PJW, Hanefeld F, Frahm J. **Proton MRS in Pelizaeus-Merzbacher disease.** *Neuropediatrics* 1997;23:355-356
 44. Pan WP, Hetherington HP, Vaughan JT, Mitchell G, Pohost GM, Whitaker JN. **Evaluation of multiple sclerosis by ¹H spectroscopic imaging at 4.1 T.** *Magn Reson Med* 1996;36:72-77
 45. Lopez-Villegas D, Lenkinski RE, Wehrli SL, Ho W-Z, Douglas SD. **Lactate production by human monocytes/macrophages determined by proton MR spectroscopy.** *Magn Reson Med* 1995;34:32-38